

*Cards*



NASA CR-54406  
Series 6, Issue 16

FACILITY FORM 602	N65-24388 (ACCESSION NUMBER)	_____
	31 (PAGES)	1 (THRU)
	CR-54406 (NASA CR OR TMX OR AD NUMBER)	26 (CODE)
		26 (CATEGORY)

QUARTERLY PROGRESS REPORT:  
INVESTIGATION OF KILOVOLT ION SPUTTERING

by

HAROLD P. SMITH, JR. AND F. C. HURLBUT

prepared for

NATIONAL AERONAUTICS AND SPACE ADMINISTRATION

CONTRACT NAS 3-5743

GPO PRICE \$ \_\_\_\_\_

OTS PRICE(S) \$ \_\_\_\_\_

Hard copy (HC) \$2.00

Microfiche (MF) .50

SPACE SCIENCES LABORATORY  
UNIVERSITY OF CALIFORNIA, BERKELEY

QUARTERLY PROGRESS REPORT:

INVESTIGATION OF KILOVOLT ION SPUTTERING

by

Harold P. Smith, Jr., and F. C. Hurlbut

prepared for

NATIONAL AERONAUTICS AND SPACE ADMINISTRATION

April 30, 1965

Distribution of this report is provided in the interest of information exchange. Responsibility for the contents resides in the author or organization that prepared it.

CONTRACT NAS 3-5743

Technical Management  
NASA Lewis Research Center  
Cleveland, Ohio

Electric Propulsion Office  
Mr. J. A. Wolters

SPACE SCIENCES LABORATORY  
University of California, Berkeley 94720

## TABLE OF CONTENTS

Abstract .....	i
Introduction .....	1
I. 1 to 10 KeV Cesium Ion Sputtering of Monocrystalline Copper .....	2
A. Introduction .....	2
B. Experimental Technique .....	3
C. Results and Discussion .....	9
1. Sputtering Yield .....	9
2. Angular Distribution .....	11
II. Mercury Ion Sputtering .....	22
III. Velocity Spectrum Measurement .....	24
IV. Measurement of Aluminum Sputtering by Neutron Activation Analysis .....	26

### FIGURES:

- Figure 1. Schematic of the combined ion source and target apparatus.
- Figure 2. Schematic diagram of target-collector assembly for measurement of the yield and angular distribution of sputtered copper. Detection of a sticking probability less than one is depicted.
- Figure 3. Sputtering yield versus incident ion energy for 1-10 KeV cesium ion bombardment normal to the (100) surface of copper at 20° C.
- Figure 4. Schematic diagram of angular collection positions.  $\theta$  is the polar angle taken equal to zero along the surface normal while  $\phi$  is the azimuthal angle measured as shown in the surface plane. The solid angle in ster-radians is presented for each collector position.
- Figure 5A - 5E. (001) polar stereographic projection of cesium-copper sputtering angular distribution for ion bombardment parallel to the surface normal and to the [001] direction. The small circles, with diameter proportional to angular emission, are placed according to their respective positions on the stereographic plot.
- Figure 6. Angular emission, normalize to isotropic emission, parallel to the  $\langle 100 \rangle$ ,  $\langle 110 \rangle$ ,  $\langle 111 \rangle$  directions as a function of energy. The lines serve only to connect points along the same direction and do not reflect any theoretical model.

QUARTERLY PROGRESS REPORT:

INVESTIGATION OF KILOVOLT ION SPUTTERING

by

Harold P. Smith, Jr. and F. C. Hurlbut

Space Sciences Laboratory, University of California, Berkeley

ABSTRACT

24388

A radioactive tracer technique has been developed and successfully applied to the measurement of the yield and angular distribution of copper sputtered from a monocrystalline target under bombardment by a 1 to 10 KeV cesium ion beam with the beam parallel to the  $\langle 100 \rangle$  crystallographic vector. The yield is seen to reach a maximum at 7 KeV and is considerably lower than that reported for polycrystalline targets. The relative openness of the (100) face is the probable reason for the significant reduction. A possible application of this effect to ion rocket electrode design is noted. The angular distribution as a function of energy is presented. Preferred ejection in the  $\langle 100 \rangle$  and  $\langle 110 \rangle$  directions as well as in the  $\{111\}$  planes is noted. A comparison of the angular distribution with energy of the incident ion is presented and discussed.

Further progress in the development of a mercury ion sputtering apparatus and in the time-of-flight velocity spectrum technique is presented. Finally, a suitable collector for activation analysis of sputtered aluminum has been tested and found satisfactory.

*Author*

## INTRODUCTION

Sputtering or ionic erosion of the accel electrode and focusing structure of the ion rocket engine can be the dominant mechanism limiting long term operation of the engine. Although the field of sputtering has been known since the phenomenon of gas discharge was first observed, no reliable theory to predict the yield, angular distribution, and velocity spectrum has been developed. Furthermore, it has only been within the past few years that experiments have been made under suitably defined conditions. In addition, there has been little work with either cesium or mercury beams so that it is difficult to predict the electrode erosion on the basis of previous data. For these reasons, the Lewis Research Center has sponsored detailed investigation of the sputtering of copper and molybdenum crystals under cesium and mercury ion beam bombardment where the target parameters such as temperature, angle of incidence, etc., are well known and varied over the range of interest.

The University of California (Berkeley) Space Sciences Laboratory began an investigation of this field early in 1964. Four vacuum systems have been constructed to study these effects using radioactive tracer techniques and activation analysis to measure the yield and angular distribution and mass spectrographic and time-of-flight analysis to determine the velocity spectrum of the various sputtered particles.

This document is submitted as a progress report on our continuing effort to develop suitable and versatile apparatus for measurement of these phenomena.

# I. 1 TO 10 KeV CESIUM ION SPUTTERING OF MONOCRYSTALLINE COPPER\*

## A. Introduction

Although sputtering has been known and investigated for almost a century, interest continues today at a high level as a result of the improved methods now available in high vacuum technology and surface physics. Equal impetus for continued study also rests in the practical value, or high nuisance value, of the sputtering phenomenon. It is the latter case that applies to the recent interest in cesium ion sputtering of conductors, especially copper. The major factor presently limiting the operational lifetime of deep probe electrostatic propulsion thrusters, or ion rockets, is the sputtering erosion by the propellant particles of the accelerator electrode system. It is hoped that a more thorough understanding of the sputtering process involving heavy alkali ion sputtering of conductors will provide, in addition to useful fundamental data, techniques to reduce or eliminate undesirable sputtering in ion rockets.

The preponderance of previous sputtering data has been concerned with the yield (atoms ejected from the solid surface per bombardment ion) and to a lesser extent with the angular distribution of the sputtered particles. The overwhelming choice of target material has been copper, while the most common ions have been those of the noble gases, particularly argon. Within the past few years, considerable progress has been made by using monocrystalline targets in preference to polycrystalline targets, since the latter obscure some of the essential features of the energy transfer process.

In this paper we will present our development of a radioactive tracer technique to measure both the yield and angular distribution of

---

\*The work reported in this section was performed by N. T. Olson and H. P. Smith, Jr.

cesium ion sputtered copper. The initial measurements, using this technique, have been made for normal bombardment of the (100) face of a monocrystalline copper target held at 20<sup>o</sup> C. The energy of the ion beam was varied from 1 to 10 KeV, corresponding to those energies most suited for proposed ion rocket missions.

#### B. Experimental Technique

Radioactive tracer techniques have been used previously in sputtering measurements. O'Brian, Lindner, and Moore,<sup>1</sup> and Gronlund and Moore<sup>2</sup> measured the yield of polycrystalline silver by radiation detection of the silver sputtered from a neutron activated target. Patterson and Tomlin<sup>3</sup> extended this technique to measurements of the angular distribution of sputtered material from a polycrystalline target. Nelson and Thompson<sup>4</sup> have made extensive use of neutron activation of the sputtered material rather than using a radioactive target in a number of excellent measurements of both yields and angular distributions. Since activation of the target before ion bombardment, rather than activation of the sputtered particles (and associated collector) following ion bombardment, has the advantage of increased sensitivity in the case of copper and other long lived isotopes, we have chosen to extend the former technique to single crystals for angular distribution measurements.

The experimental apparatus consists of a large target chamber evacuated by a cryogenically baffled oil diffusion pump and an ion source chamber with a 200 liter/sec vac-ion pump (see Figure 1). Metal gaskets

- 
1. C. D. O'Brian, A. Lindner, and W. J. Moore, J. Chem. Phys. 29, 3 (1958).
  2. F. Gronlund and W. J. Moore, J. Chem. Phys. 32, 1540 (1960).
  3. H. Patterson and D. H. Tomlin, Proc. Roy. Soc. 265A, 474 (1961).
  4. R. S. Nelson and M. W. Thompson, Proc. Roy. Soc. 259A, 458 (1961).

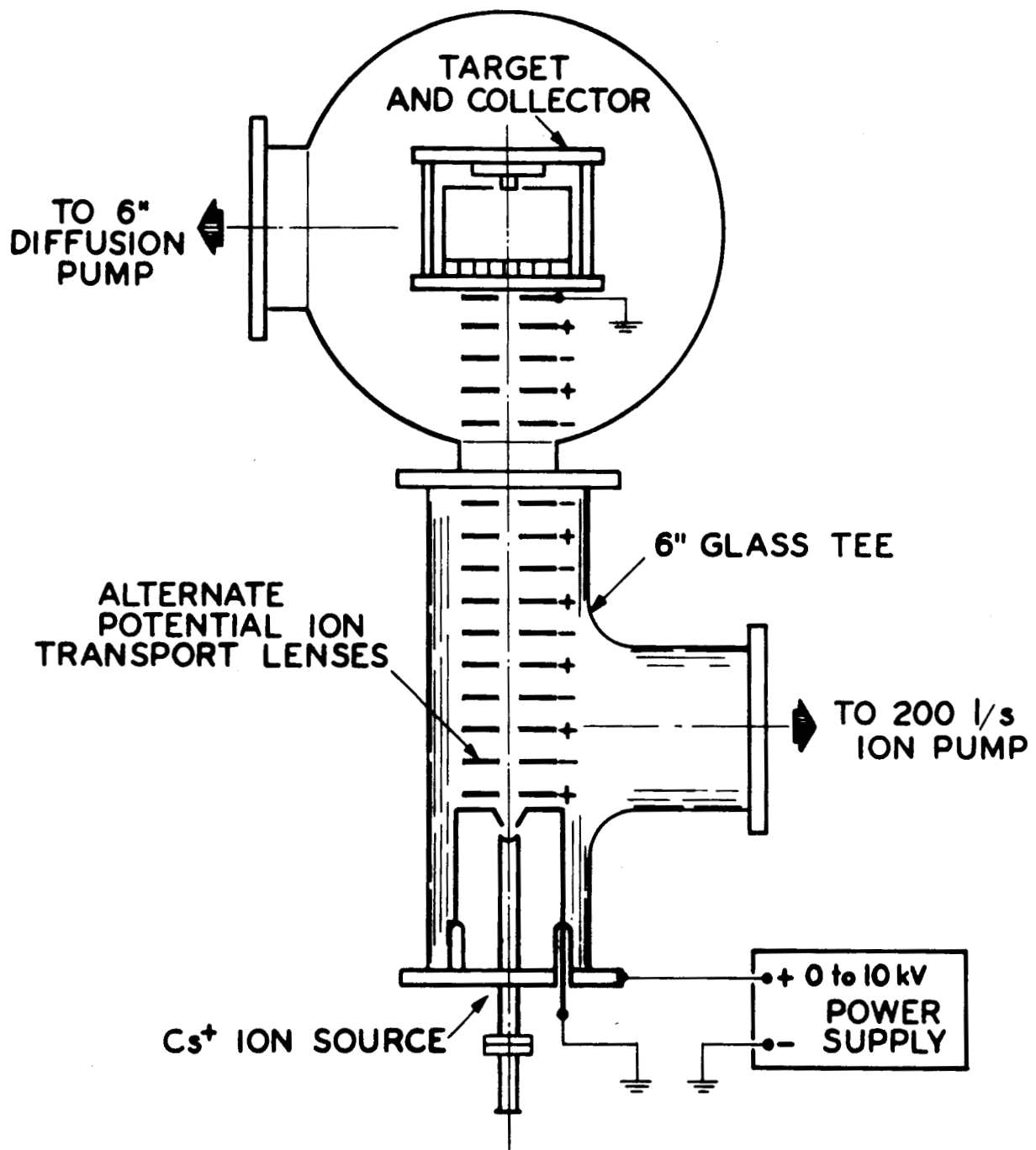


Figure 1. Schematic of the combined ion source and target apparatus.



are used exclusively in the target chamber while viton o-rings are used for three ports on the source chamber. The base pressure of both systems was  $2 \times 10^{-8}$  torr without recourse to baking. During ion beam operation, the pressure was  $1.5 \times 10^{-7}$  torr in the source chamber and  $1.5 \times 10^{-7}$  torr or lower in the target chamber.

A porous tungsten-surface ionization cesium ion source was operated at 1 to 10 KeV and insulated from the target chamber by the glass tee. When used in conjunction with an alternating potential electrostatic focusing system, the source provided 10 to 20  $\mu$ a at the target surface. Since the measured target cross-section of the beam was  $0.7 \text{ cm}^{-2}$ , sputtering took place under clean surface conditions (see Yonts and Harrison<sup>5</sup>).

The maximum sensitivity of the radioactive tracer technique is determined by the saturation activity that can be induced in the particular material. However, the radiological hazard involved in handling the copper specimens precluded activation to saturation. The practical maximum sensitivity is thus set by the maximum activity that can be reasonably handled. Thus, the smaller the total target weight, the higher the specific activity (curies/gm) and the higher the detection sensitivity.

To prepare as small a target as possible, a thin wafer (0.030 in.) was spark cut from a 3/4 inch diameter single crystal copper rod. The wafer was chemically and then electrically polished to a thickness of 0.005 inches. This method of preparation leaves crystal structure undisturbed.

Following preparation, the crystallographic orientation of the target was measured by Laue-back X-ray diffraction. A high purity aluminum holder was then constructed to insure alignment to within  $1^\circ$  with

---

5. O. C. Yonts and D. E. Harrison, Jr. J. Appl. Phys. 31, 1583 (1960).

the  $\langle 100 \rangle$  direction.

The target was irradiated in a thermal neutron flux of  $5 \times 10^{12}$  neutrons  $\text{cm}^{-2} \text{sec}^{-1}$  for 15 minutes. Neutron capture by  $\text{Cu}^{63}$  (69% abundant) produced  $\text{Cu}^{64}$  which is positron unstable and decays with a half-life of 12.9 hours. This induced activity allowed measurement of 0.1 micrograms of sputtered material.

The collector assembly consisted of a square base fabricated from 100 aluminum cubes (1.1 cm on a side) which were arranged 10 on a side. The assembly was placed opposite the target face (see Figure 2) and provided the means for separating the collector so that quantitative angular distribution measurements were possible. After sputtering the target with Cs ions, the cubes were removed and analyzed to determine the radioactivity of each collector; thus providing a relative measure of the amount of copper collected on each cube.

To complete the total yield measurement, the  $10 \times 10$  collector was surrounded with aluminum foil sides and a bottom foil, thereby enclosing the  $2\pi$  steradians above the target. As can be seen from Figure 2, the bottom foil collector should not directly intercept any sputtered copper. However, for all experiments it collected 3% or less of the total amount. From this, we conclude that the sticking probability of the sputtered copper on the aluminum was very close to one. In addition, shadow measurements of evaporated copper on aluminum were made to insure that surface migration of copper on the aluminum collectors was insignificant.

The radioactivity of the collector cubes and foils was measured by using a shielded gamma ray spectrometer which discriminates against all background except that associated with the 511 KeV positron

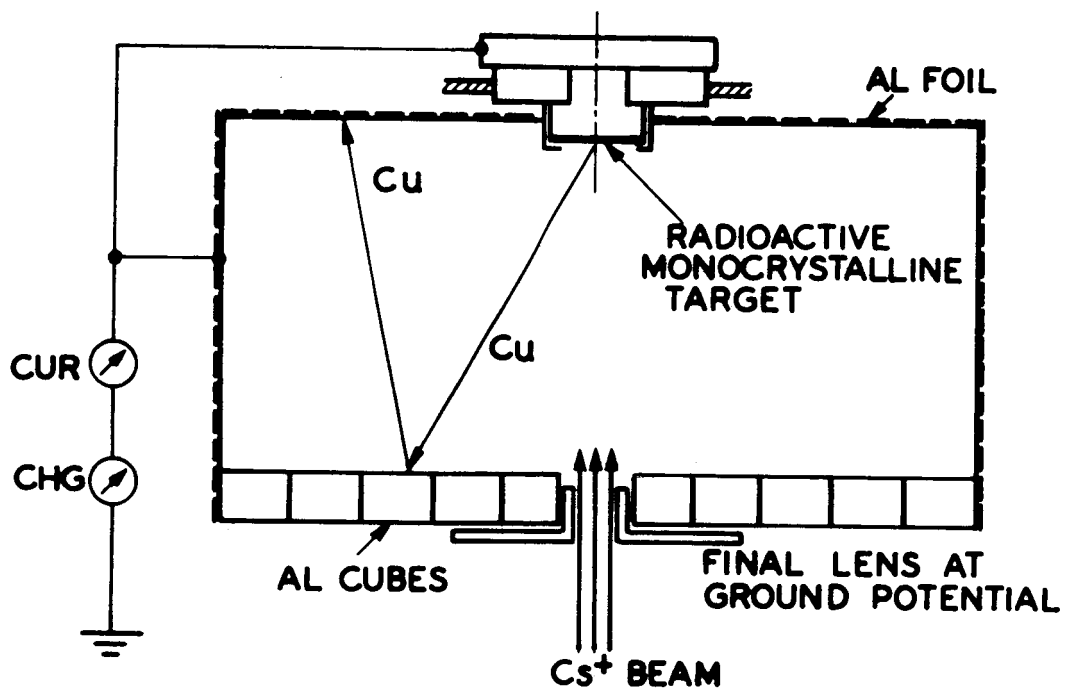


Figure 2. Schematic diagram of target-collector assembly for measurement of the yield and angular distribution of sputtered copper. Detection of a sticking probability less than one is depicted.

annihilation gamma radiation. All background that varies in a linear manner with energy in those channels associated with the peak in question was eliminated by computing the number of counts by Covell's method.<sup>6</sup> Absolute measurement of the amount of copper on each collector surface was made by direct comparison with the radioactivity of a known weight of copper irradiated with the target. Hence, the absolute angular distribution throughout a large part of the hemispherical solid angle above the target can be directly inferred from the activity of each collector block. The total number of atoms sputtered is clearly computed from the sum of the activity of all collector pieces. The rather laborious process of counting and correcting for radioactive decay with time is circumvented by use of an automatic sample changer with output directly usable for digital computer data reduction.

In order to determine the yield, it was necessary to measure the total number of ions striking the target. This was accomplished by summing and integrating the current to the target and collector assembly which serves as a simplified Faraday cage as shown in Figure 2. Preliminary measurements were made to insure that the ion beam did not strike the collector when entering the assembly and that beam divergence after entering was not sufficient to spread the beam to a wider cross sectional area than the target. Summation of the target and collector currents removes any inaccuracy associated with secondary and photoelectron production in the assembly. Further measurements were made to insure that the ion beam was not contaminated by secondary electrons created in the lens structure by ion bombardment.

---

6. D. F. Covell, U. S. Naval Radiological Defense Laboratory, Mare Island, Calif., Tech. Report 288.

## C. Results and Discussion

### 1. Sputtering yield

The yield or sputtering coefficient  $S$  is shown as a function of incident ion energy in Figure 3. The reproducibility of the points was within five percent. The general shape of the yield curve compares favorably with the extensive cesium sputtering of polycrystalline targets (excluding copper) by Lebedev, Stavisskii and Shut'ko<sup>7</sup> who also noticed a maximum in the yield curves in the neighborhood of 7 KeV. However, the actual values are considerably below those of Almen and Bruce<sup>8</sup> who measured a 45 KeV cesium-copper sputtering yield of 15. It is unlikely that the lower value is associated with the initial presence of a tenacious surface layer such as copper oxide since over 1000 monolayers were sputtered during each measurement. This contention is supported by the measurements of Almen and Bruce<sup>9</sup> who showed that xenon-copper sputtering yield is constant after  $100 \mu\text{g}/\text{cm}^2$  have been removed. We were well above this limit. It is more likely that the low value of yield is associated with the alignment of the ion beam parallel to the  $\langle 100 \rangle$  axis of the crystal target, rather than the random alignment that was the case in the Almen and Bruce cesium-copper data.

There have been a number of measurements of noble gas ion-single crystal copper sputtering that show a wide variance of yield depending on the crystal orientation. Almen and Bruce<sup>8</sup> found a change from 10 to 30 by rotating the target from parallel alignment of the  $\langle 100 \rangle$  axis with a 45 KeV krypton ion beam through  $7^\circ$ . Similarly, Southern,

---

7. S. Y. Lebedev, Y. Y. Stavisskii and Y. V. Shut'ko, Soviet Physics - Tech. Physics, 9, 6 (1964).

8. O. Almen and G. Bruce, Nucl. Inst. and Methods 11, 279 (1961).

9. O. Almen and G. Bruce, Nucl. Inst. and Methods, 11, 257 (1961).

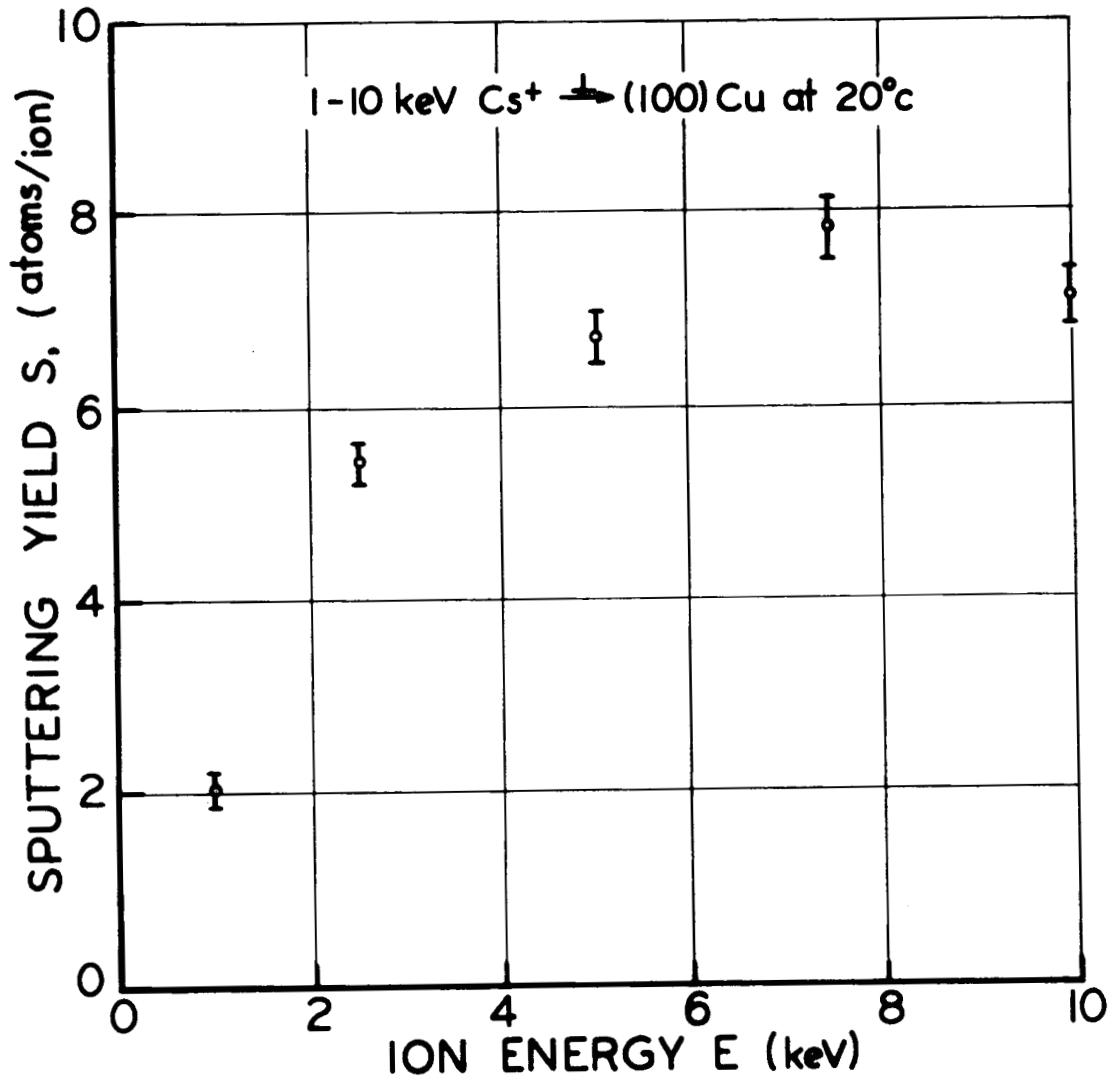


Figure 3. Sputtering yield versus incident ion energy for 1-10 KeV cesium ion bombardment normal to the (100) surface of copper at 20°C.

Willis, and Robinson<sup>10</sup> found a factor of two variation in 1-5 KeV argon-copper sputtering by changing the angular orientation of the target with respect to the beam. A variable parameter first collision model that considered the relative openness of the low index crystallographic directions compared favorably with their results. Hence, the low yield values reported in this paper probably reflect the alignment of the beam with the low index  $\langle 100 \rangle$  direction. Further measurements will be made to note the effect of slightly off-axis alignment.

The large variance in sputtering yield that can be expected with single crystals suggests the possibility of manufacturing ion rocket electrodes from a highly cold worked material with a resultant preferred alignment of the crystallites. If charge exchange ions, which are primarily responsible for the ion rocket electrode damage, attack the electrode along parallel paths, it may be possible to significantly reduce the sputtering damage by proper orientation of the preferred crystallographic direction with respect to the ion path.

## 2. Angular Distribution

The angular distribution of sputtered particles, resulting from ion bombardment parallel to the target surface normal and to the  $\langle 100 \rangle$  crystallographic direction, should exhibit a fourfold crystal symmetry. Since our data was taken using a square array symmetrically centered above the surface, we should obtain a fourfold degeneracy in the angular distribution independent of the azimuthal orientation of the crystal. This symmetry was observed. The standard deviation from the calculated mean of each of the 25 non-degenerate collector positions

---

10. A. L. Southern, R. Willis, and M. T. Robinson, J. Appl. Phys. 34, 153 (1963).

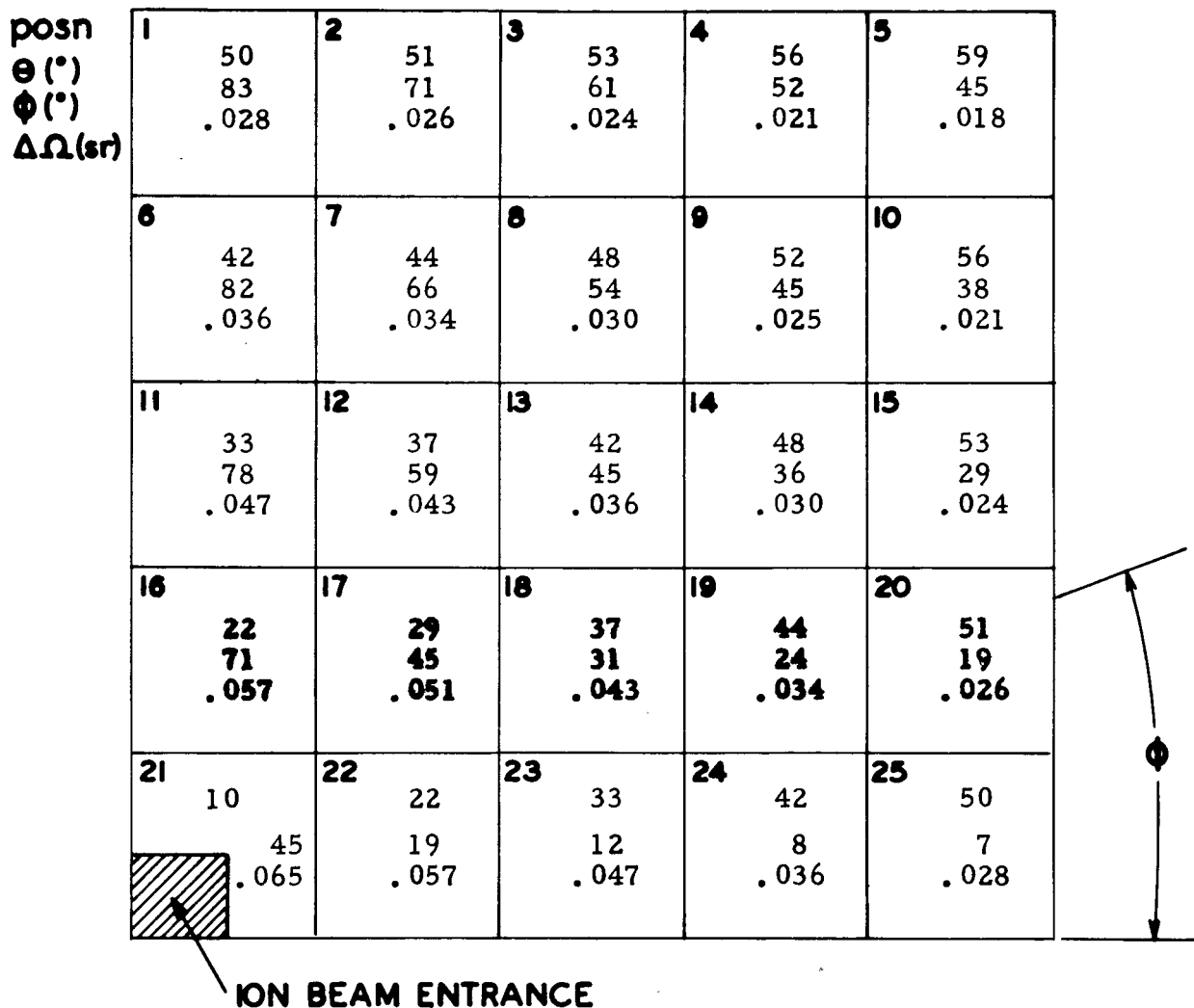


Figure 4. Schematic diagram of angular collector positions.  $\theta$  is the polar angle taken equal to zero along the surface normal while  $\phi$  is the azimuthal angle measured as shown in the surface plane. The solid angle in steradians is presented for each collector position.



was determined by standard formulae and showed that fourfold symmetry was always present with less than 10% deviation from any mean value.

The relative angular distribution is presented in tabular form in Table I where the collector positions can be deduced by reference to Figure 4. The value for each position gives the emission per unit solid angle normalized to isotropic emission. In our particular apparatus the solid angle intercepted by the collector blocks varied from 0.065 sr near the normal to 0.018 sr near the edge. As can be seen from Figure 4, the planar angle divergence at a polar angle  $\theta = 45^\circ$  (the polar angle of the close packed  $\langle 110 \rangle$  direction) is of the order of  $10^\circ$ . Although our angular resolution of  $10^\circ$  is essentially equal to the full angular width at half maximum reported by Molchanov and Tel'kovskii<sup>11</sup> for focused emission in the  $\langle 110 \rangle$  direction and is satisfactory for the discussion presented below, the advantage of a finer collection grid is readily apparent. The additional accuracy can be obtained by placing all 100 collectors in a single quadrant and invoking the symmetry property. The resolution would then be increased by a factor of four over the present data. Furthermore, the resolution could again be doubled by noting the mirror symmetry of the crystal along  $\{110\}$  and  $\{100\}$  planes intercepting the  $\{100\}$  surface.

A schematic representation of the angular distributions at each energy is presented in Figures 5A through 5E. Each of the 25 non-degenerate angular collectors are positioned according to a standard stereographic polar projection of the (001) crystallographic face. A circle with diameter proportional to the relative angular emission is

---

11. V. A. Molchanov and V. G. Tel'kovskii, Bull. Acad. Sci. USSR, Phys. Ser. (USA), 26, 1470 (1963).

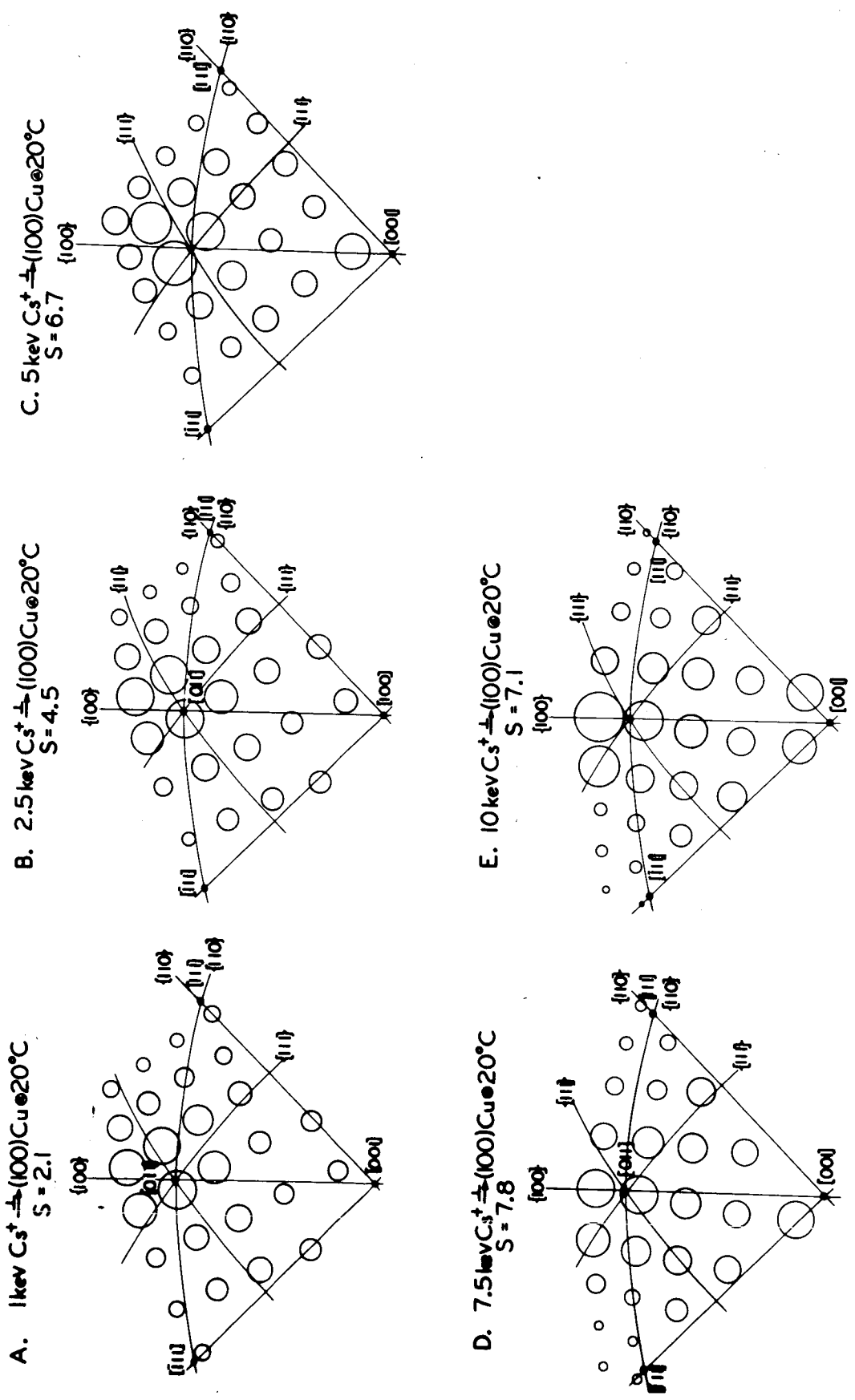


Figure 5A - 5E. (001) polar stereographic projection of cesium-copper sputtering angular distribution for ion bombardment parallel to the surface normal and to the [001] direction. The small circles, with diameter proportional to angular emission, are placed according to their respective positions on the stereographic plot.

then drawn about the midpoint of each angular collector position. The preferred ejection in the  $\langle 110 \rangle$  and  $\langle 100 \rangle$  directions as well as in the  $\{111\}$  planes can be noted and is in agreement with other investigations.<sup>4,10,12</sup> In addition, it can also be seen that ejection in the  $\{100\}$  plane at polar angles greater than  $45^\circ$  (angles greater than the  $\langle 110 \rangle$  direction) is preferred over ejection at angles less than  $45^\circ$ .

Change in the angular distribution with incident ion energy should offer the possibility to investigate the importance of focused momentum propagation in the sputtering process. This contention can be based on the calculations of Gibson, Goland, Milgram, and Vineyard<sup>13</sup> who have shown that the momentum of lattice atoms following the creation of a primary knock-on far from any surface tends to propagate primarily in the focusing directions after the momentum has been transported beyond a few nearest neighbor distances from the primary event. Furthermore, energy is propagated with high efficiency of 2/3 eV loss per collision in a perfectly focused copper chain at absolute zero. Silsbee<sup>14</sup> has concluded that thermal motion should not greatly affect the energy loss per collision so that efficient propagation can be expected at the temperatures at which our data was taken. However, it should be noted that Nelson, Thompson, and Montgomery<sup>15</sup> and Sanders and Fluit<sup>16</sup> have suggested that focused propagation is measurably affected by thermal vibrations. Hence, direct application of the Gibson, et. al. results for 400 eV primary knock-ons at  $0^\circ$  K may be misleading. However, there is ample evidence\* that significant energy transfer

---

12. R. L. Cunningham, K. V. Gow, and J. Ng-Yelim, J. Appl. Phys. **34**, 984 (1963).

13. J. B. Gibson, A. N. Goland, M. Milgram, and G. H. Vineyard, Phys. Rev. **120**, 1229 (1960).

14. R. H. Silsbee, J. Appl. Phys., **28**, 1246 (1957)

15. R. S. Nelson, M. W. Thompson, H. Montgomery, Phil. Mag. **7**, 1385 (1952).

16. J. B. Sanders and J. M. Fluit, Physica **30**, 129 (1964).

\*The latest in a long series of investigations of heavy ion penetration is reported by Kornelson, Brown, Davies, Domeij and Percy, Phys. Rev. **136A**, 849 (1964).

A review of much of the past work in heavy ion penetration is presented therein.

collisions between the incident ion and the lattice atom occur at greater depths into the lattice as the incident ion energy is increased. Hence, one can infer from the Gibson, et. al. results that the only means by which cesium-copper collisions at depths exceeding a few lattice constants can contribute to sputtering is by focused momentum (and possibly mass) transport to the surface. Sputtering events created by a process of this nature should lead to emission closely parallel to the focused directions. Hence, increased focused emission with increased incident ion energy should imply that focused chains play a significant role in the sputtering phenomenon. Conversely, the absence of a strong proportional dependence of focused emission and ion energy should imply that only the first few monolayers of the lattice contribute to sputtering. Since geometrical considerations show that very short chains of hard sphere collisions in the first two monolayers of a (100) surface can lead to preferred ejection near the  $\langle 110 \rangle$  direction, the presence of preferred ejection, even in the focusing directions, does not necessarily imply that long (greater than ten) collision chains exist. But, if the amount ejected parallel or nearly parallel continually increases with ion energy, then one concludes that a significant number of long collision chains lead to sputtering.

The practical result of considerations of this nature follows. If long collision chains are primarily responsible for sputtering, then the yield can be reduced by blocking the focused momentum process. One method by which this could be accomplished would be the use of binary interstitial alloys of significant mass difference since the relative momentum loss even in perfectly focused chains would be equal to  $\left| \frac{M-1}{M+1} \right|$  per collision where M is the mass ratio of the alloying species. However,

if long collision chains are not of primary importance, binary alloying may not decrease and could possibly increase the sputtering yield.

Figure 6 presents the relative angular emission in the  $\langle 100 \rangle$ ,  $\langle 110 \rangle$ , and  $\langle 111 \rangle$  directions as a function of incident ion energy. Emission in the close-packed  $\langle 110 \rangle$  direction is independent of energy while emission in the  $\langle 100 \rangle$  direction increases with energy between 1 and 5 KeV, but is constant thereafter. Emission in the  $\langle 110 \rangle$  direction is always greater than that associated with isotropic emission (i. e.  $\frac{\Delta s}{\Delta \Omega} / \frac{s}{2\pi} = 1$ ) or with emission proportional to the cosine of the polar angle.\*

Similarly, emission along the  $\langle 100 \rangle$  direction is also greater than isotropic. It should be noted that simultaneous measurement of both the yield and angular distribution is necessary in order to compare the measured results with isotropic emission.

Southern, Willis, and Robinson<sup>10</sup> noticed a qualitatively similar effect with argon-copper sputtering in the 1 to 5 KeV region. Although a larger energy range would be of assistance in interpreting these results, the insensitivity to energy of  $\langle 110 \rangle$  emission suggests that the length of the close-packed chains is short in comparison to the penetration of the cesium ion and that only those chains initiated in the first few monolayers yield a sputtered particle.

The rise in  $\langle 100 \rangle$  emission with energy is more perplexing. Nelson and Thompson pointed out that focusing in this direction in

---

\* If  $N_0$  atoms/cm<sup>2</sup> are sputtered, an exact cosine distribution would yield  $\frac{N_0 \cos \theta}{\pi}$  atoms/cm<sup>2</sup> per unit solid angle or  $2 \cos \theta$  normalized to isotropic emission. Although some angular sputtering data from polycrystalline targets approximate a cosine distribution, the result is probably fortuitous and there appears to be no clear reason to expect monocrystalline data to conform to this distribution.

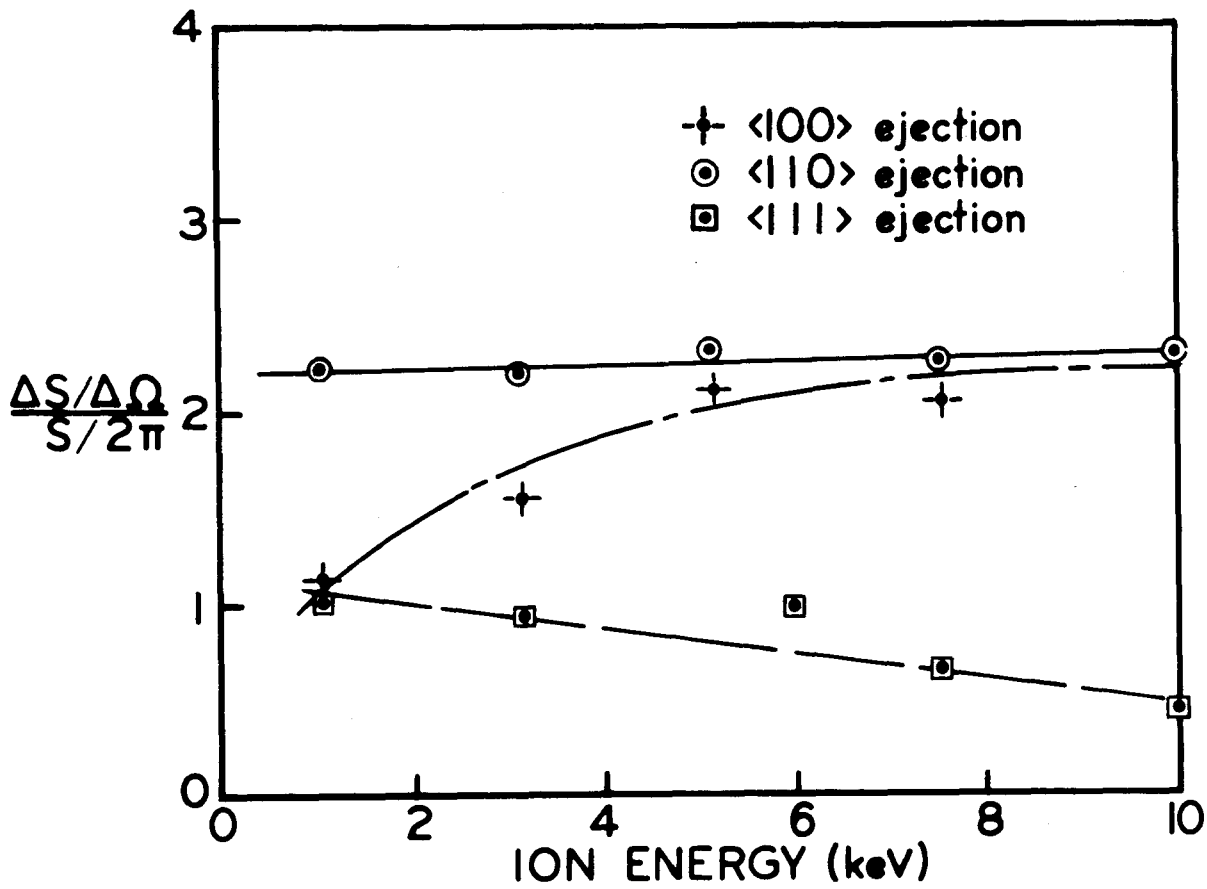


Figure 6. Angular emission, normalize to isotropic emission, parallel to the <100>, <110>, <111> directions as a function of energy. The lines serve only to connect points along the same direction and do not reflect any theoretical model.

fcc requires interaction with neighboring chains ("assisted focusing") with a consequent greater energy loss per collision than in the case of close-packed focusing where interaction is slight. This contention has been corroborated by the calculations of Gibson, et. al. The lower efficiency of the  $\langle 100 \rangle$  chain may account for the initial increase in emission with energy, but any definite conclusion in this regard will have to await computer simulation of sputtering in a manner similar to their work.

The  $\langle 111 \rangle$  vector is a non-focusing direction in fcc as a result of large atomic separation in the chain and asymmetry with respect to the neighboring chains. Hence, emission in this direction as a function of ion energy may be taken as a measure of unfocused sputtered ejection. A discernable, although not large decrease in  $\langle 111 \rangle$  emission with ion energy can be noted in Figure 6. It is possible that this decrease can be associated with the increased emission in the  $\langle 100 \rangle$  direction. Neither the angular resolution nor the range of ion energy is sufficient for definite conclusions to be drawn with regard to energy dependent focused emission. However, it does appear that non close-packed focusing increases with ion energy although only as a weak function of the larger variations of ion energy and resultant deeper lattice penetration.

In a similar vein, the present resolution is not suitable for a detailed investigation of emission in the  $\{111\}$  planes, a qualitative effect noticed by others<sup>4,12</sup>. It is clear that the effect is also present in our data, but its dependence on energy cannot be clearly discerned. Emission in the  $\{111\}$  plane is in agreement with some preliminary computer simulation of copper sputtering.<sup>17</sup>

---

17. Private communication: D. E. Harrison, Jr.

Preferred emission which is further enhanced by increased ion energy can be noted in the  $\{100\}$  plane at polar angles greater than  $45^\circ$ . Southern, Willis, and Robinson<sup>10</sup> noticed that argon sputtered copper emission in the  $\langle 110 \rangle$  direction was skewed towards smaller polar angles rather than larger angles as we find. They attributed this to the repulsive asymmetry in the surface force field at the end of a fully focused close-packed chain. They also pointed out that focused ejection at smaller angles could be attributed to the greater distance between the first two monolayers than the bulk spacing between (100) layers. Obviously, neither of these mechanisms can account for the larger polar angles that we find with cesium-copper sputtering.

It is our contention that fully focused chains rarely lead to a sputtering event. This is in agreement with very recent computer simulation of cesium-copper sputtering by R. N. Schlaug<sup>18</sup> who noticed that collision chains leading to sputtering were usually less than five and only very rarely greater than ten. If this is the case, it is unlikely that well focused chains lead to a sputtering event. Furthermore, it can be conjectured in a qualitative sense that skewed  $\langle 110 \rangle$  emission towards polar angles further from the surface normal can result from the inability of short collision chains to completely rotate the original momentum vector associated with the cesium ion through the  $135^\circ$  associated with emission in the  $\langle 110 \rangle$  direction.

It is hoped that agreement between angular data of the type presented above, especially with improved angular resolution, to computer simulation of cesium-copper sputtering in a manner similar to that of

---

18. R. N. Schlaug, Ph. D. Thesis, Department of Nuclear Engineering, University of California, Berkeley, California



Gibson, et. al. will offer a suitable test for proposed interatomic potentials for copper-copper collisions as well as cesium-copper collisions and thereby lead to a full understanding of sputtering. Recent work by Harrison and Schlaug suggest that such detailed comparison may soon be available.

## II. MERCURY ION SPUTTERING\*

Construction and assembly of apparatus for mercury ion sputtering similar to that used for cesium ion sputtering is in process. This apparatus is, of necessity, more complex than the cesium apparatus as a result of the formation of multiple charged mercury ions and contaminant ions in the electron bombardment ion source. In order to insure that only singly charged (or only doubly charged) mercury ions of known energy strike the target, it is necessary to pass the ion beam through a bending magnet.

The mercury ion source has been mounted and found to operate satisfactorily between 1 and 10 KV. Eventual operation at 20 KV is planned. Beam currents up to 700  $\mu$ a have been attained. A considerable amount of time has been spent in testing the effect of various parameters on source operation. These have included variation of the arc voltage, electron emission current, reservoir temperature (neutral flow rate), and extractor voltage. During operation, the source chamber operated at pressures lower than  $6 \times 10^{-6}$  torr without cryogenic cooling in the source chamber. Provision has been made for such cooling in order that during actual investigation of sputtering the ion source will offer as low a pressure contaminant as possible in the target chamber which is differentially pumped. Our experience to date indicates that the source is satisfactory for the intended measurements.

A magnet, suitable for bending the mercury beam, has been delivered and tested. Some alteration of the pole pieces was required before acceptance could be made. It is not expected that this will cause a significant

---

\*The work reported in this section was performed by R. G. Musket

delay in the program.

It is expected that work in the next quarter will include investigation of beam transport and magnetic bending. No problems are envisioned in the technique of measurement of mercury ion sputtering yield and angular distributions since the method will be analogous to that reported in Section I.

### III. VELOCITY SPECTRUM MEASUREMENT\*

In performing an analysis of the velocity spectrum of sputtered particles the parent ion beam is first modulated by electrostatic deflection transverse to a slit system and then allowed to impinge on a target as a series of discrete pulses. Assuming that the time lapse in sputtering is of negligible magnitude in comparison with flight times of the sputtered particles and that the flight time lapse from modulator to target is also short and known, spectra of arrival times of sputtered particles of a detector are immediately translatable into spectra of velocities for those particles. The analysis proceeds straight forwardly if the parent ion beam is monoenergetic. The elements of an arrival time analysis system are: 1. modulator, 2. ionizer, 3. spectrometer, 4. multiplier detector, 5. signal amplifier train, 6. data acquisition system. Progress in the last quarter in the development and testing of each of these system elements is indicated in the following.

An electrostatic deflection modulator has been constructed and tested. Although the time response characteristics of this present design are satisfactory, about 1% transmission was observed in the "cut-off" condition. Redesign is in process, with completion of a satisfactory modulator projected for the coming quarter. A modulator drive supply has been constructed and will be tested when the new modulator becomes available.

The spectrometer-ionizer-detector system, from all present indication, would seem to be functioning acceptably. Detected particles appear as current pulses of approximately 50 n-sec total duration with

---

\*Work reported in this section was performed by D. W. Demichele, F. C. Hurlbut, and H. P. Smith, Jr.

rise times of about 30 n-sec. These relatively long rise times are evidence of response time limitations in the amplifier train. A new and faster preamplifier has been constructed. The outcome of work to date may be summarized by indicating that pulses originating in the detector due to individual ions of arbitrary species may be resolved and indicated on an oscilloscope screen or may be counted in a data acquisition system. The quadrupole spectrometer is working well although some interference in the signal train was produced by the spectrometers three megacycle r. f. signal. Installation of a suitable filter has eliminated the problem.

Pulse arrival rates anticipated in velocity analysis investigation are consistent with information storage by means of 10 mc counting equipment. At present the Techronix 547 delayed gate system will provide a variable position information channel through which signal data will flow. In a parallel development in the Aerosciences Division (ME) an EH gate generator has been purchased and will become a portion of a gated current-integration arrival-time analyzer. This work, which is being performed under other support, is under the direction of F. C. Hurlbut. A close working relationship has been established with the ME group and a beneficial exchange of information is taking place. Dr. Paul Scott, currently on leave from M. I. T., is participating. Thus a comparative study of pulse-counting and current-integrating types of analysis systems is anticipated in the forthcoming quarter.

#### IV. MEASUREMENT OF ALUMINUM SPUTTERING BY NEUTRON ACTIVATION ANALYSIS\*

Thin lead foils have been obtained in which the aluminum impurity is less than 0.2 micrograms. Neutron activation analysis of the foils shows that the only contaminant contribution to the  $^{28}\text{Al}$  photopeak is very long lived and that the amount of this contamination is small in comparison to 1 microgram of aluminum. As a result of the long half life of the contaminant, it is easily removed in a known manner by counting the foil following ten half lives of the activated aluminum isotope (i. e. waiting approximately 30 minutes after neutron irradiation). Covell's method is then suitable for obtaining both the aluminum activity and for stripping the contaminant activity from the sample. This technique has been successfully used to measure a known quantity of aluminum by neutron activation analysis. These results show that 10 micrograms could be measured with less than 5% error.

In testing, the lead foils have been subjected to the same handling that will be used for actual sputtering measurements. In addition, all foils to be used in the initial series of measurements have been irradiated to insure that the amount of aluminum and contamination in the  $^{28}\text{Al}$  photopeak is within acceptable limits. Actual measurements are planned for the latter part of May.

---

\*The work reported in this section was performed by E. H. Hasseltine

Energy (keV) $\Phi(\langle 110 \rangle)$	1 64°	2.5 64°	5 50°	7.5 7°	10 7°
position	$(\Delta s / \Delta \Omega / s / 2\pi)$				
1	1.20	1.34	1.02	1.67	1.65
2	2.15	2.11	1.11	1.02	1.11
3	2.22	2.42	1.52	.79	.79
4	1.56	1.61	1.58	.66	.38
5	1.03	1.01	1.76	.587	.52
6	1.62	1.71	1.33	1.86	1.80
7	2.48	2.44	1.84	1.18	1.19
8	2.32	2.37	2.82	.92	.98
9	1.38	1.49	2.46	.73	.85
10	.98	.91	1.41	.64	.76
11	1.58	1.68	1.67	1.82	1.92
12	1.97	2.05	1.89	1.70	1.62
13	1.83	1.73	2.38	1.40	1.45
14	1.20	1.11	1.79	1.08	1.11
15	.87	.78	1.25	1.22	.81
16	1.28	1.37	1.71	1.64	1.70
17	1.38	1.56	1.53	1.72	1.80
18	1.54	1.63	1.69	1.80	1.78
19	1.11	1.20	1.56	1.92	1.77
20	1.10	.83	1.07	2.17	2.64
21	1.24	1.54	2.18	2.11	2.19
22	1.27	1.37	1.52	1.68	1.80
23	1.53	1.43	1.55	1.91	1.96
24	1.33	1.29	1.35	2.48	2.38
25	.89	.88	.94	2.47	3.04

Table 1. Relative angular distribution normalized to isotropic emission as a function of energy. The angular position number corresponds to that shown in Figure 3. The azimuthal orientation of the  $\{100\}$  plane, which contains the close-packed  $\langle 110 \rangle$  vector, is also shown for each measurement.

QUARTERLY REPORT DISTRIBUTION LIST

Contract NAS 3-5743

<u>Copies</u>	<u>Addressee</u>	<u>Copies</u>	
2	NASA Headquarters FOB - 10B 600 Independence Ave., NE Washington, D. C. 20546 Attn: RNT/James Lazar	1	WLPC/Capt. C. F. Ellis AFWL Kirtland Air Force Base, New Mexico
2	NASA-Lewis Research Center 21000 Brookpark Road Cleveland, Ohio 44135 Attn: J. H. Childs	1	Space Technology Laboratories One Space Park Redondo Beach, California Attn: Dr. D. B. Langmuir
1	D. L. Lockwood	1	M-RP-DIR/E. Stuhlinger NASA-Marshall Space Flight Center Huntsville, Alabama 35812
5	J. A. Wolters		
1	Y. E. Strausser		
1	J. H. DeFord		
1	Tech. Utilization Office		
2	Library		
1	Reports Control Office		
1	W. Moeckel	6	NASA Scientific and Technical Information Facility Box 5700 Bethesda, Maryland 20014 Attn: NASA Rep. /RQT-2448
1	Hughes Research Laboratory 3011 Malibu Canyon Road Malibu, California Attn: Dr. G. Brewer	1	Commander Aeronautical Systems Division Wright-Patterson Air Force Base, Ohio Attn: AFAPL (APIE)/Robert Supp
1	Dr. H. Wiser		
1	Electro-Optical Systems, Inc. 125 North Vinedo Avenue Pasadena, California Attn: A. T. Forrester	1	NASA-Ames Research Center Moffett Field, California 94035 Attn: T. W. Snouse
1	Dr. D. B. Medred		
1	Litton Systems, Inc. Beverly Hills, California Attn: Dr. G. K. Wehner	1	Varian Associates 611 Hansen Way Palo Alto, California Attn: Technical Library
1	General Dynamics/Astronautics P. O. Box 1128 San Diego, California 92112 Attn: Dr. D. Magnuson	1	Astro Met Associates, Inc. 500 Glendale-Milford Road Cincinnati 15, Ohio Attn: Mr. J. W. Graham
1	Field Emission Corporation 611 Third Street McMinnville, Oregon Attn: Dr. L. W. Swanson	1	Professor Lawrence Shaffer Department of Physics Hiram College Hiram, Ohio
1	General Electric Company Flight Propulsion Laboratory Evandale, Ohio Attn: Dr. M. L. Bromberg	1	Professor J. B. Fenn Department of Aeronautical Engr. Princeton University Princeton, New Jersey